WPS1-PR(18) 20799

T Stange et al.

First Demonstration of Magnetically Confined High Temperature Plasmas beyond the X2-cutoff density sustained by O2-heating only

Preprint of Paper to be submitted for publication in
Physical Review Letters

This work has been carried out within the framework of the EUROfusion Consortium and has received funding from the Euratom research and training programme 2014-2018 under grant agreement No 633053. The views and opinions expressed herein do not necessarily reflect those of the European Commission.

First Demonstration of Magnetically Confined High Temperature Plasmas beyond the X2-cutoff density sustained by O2-heating only

T. Stange,[1,*] H. P. Laqua,[1] S. Bozhenkov,[1] K.-J. Brunner,[1] S. Marsen,[1] D. Moseev,[1] J. Baldzuhn,[1] Y. O. Kazakov,[2] U. Höfel,[1] A. Langenberg,[1] N. Marushchenko,[1] M. Beurskens,[1] R. Wolf,[1] A. Ali,[1] H. Braune,[1] N. Chaudhary,[1] H. Damm,[1] A. Dinklage,[1] P. Drewelow,[1] G. Fuchert,[1] Y. Gao,[3] O. Grulke,[1] D. Hartmann,[1] P. Helander,[1] M. Hirsch,[1] M. Jakubowski,[1] J. Knauer,[1] R. König,[1] C. Lechte,[4] H. Trimino Mora,[1] U. Neuner,[1] H. Niemann,[1] N. Pablant,[5] J. W. Oosterbeek,[1] E. Pasch,[1] B. Plaum,[4] A. Puig Sitjes,[1] K. Rahbarnia,[1] J. Schilling,[1] H. Thomsen,[1] Y. Turkin,[1] G. Wurden,[5] and the Wendelstein 7-X team[†]

[1] *Max-Planck-Institute for Plasma Physics, Wendelsteinstraße 1, 17491 Greifswald, Germany*
[2] *Laboratory for Plasma Physics, LPP-ERM/KMS, Brussels, Belgium*
[3] *Forschungszentrum Jülich GmbH, Institut für Energie- und Klimaforschung – Plasmaphysik, 52425 Jülich, Germany*
[4] *Institute for Interfacial Process Engineering and Plasma Technology, University Stuttgart, Germany*
[5] *Princeton Plasma Physics Laboratory, Princeton, NJ, USA*

(Dated: October 8, 2018)

Plasma densities well above $10^{20}\,\mathrm{m}^{-3}$ are desirable for achieving high fusion power and necessary to access the collisionality regime for which the stellarator Wendelstein 7-X was optimized. 2^{nd} harmonic electron-cyclotron-resonance heating in X-mode polarization has a single path absorption close to 100 %, but allows heating only up to a cut-off density of $1.2 \cdot 10^{20}\,\mathrm{m}^{-3}$ in contrast to the weakly absorbed O-mode with cut-off at $2.4 \cdot 10^{20}\,\mathrm{m}^{-3}$. Therefore, a triple-beam-path scenario was designed and a magnetically confined high temperate, high density plasma sustained for the first time beyond the X2-cut-off by O2-mode heating only.

PACS numbers: ... May be entered using the environment PACS numbers.

I. INTRODUCTION

Fusion experiments need to operate at high plasma density, n, because the fusion power is proportional to n^2 and the confinement usually improves with increasing n. In tokamaks, the achievable density is however constrained by the so-called Greenwald limit [1], which is proportional to the plasma current and therefore limited by instabilities. As a result, the highest-performance tokamak plasmas [2–5] are forced to operate at relatively low densities and high temperatures T far above the optimum ($\sim 10\,\mathrm{keV}$) for maximum fusion performance.

Stellarators are not subject to the Greenwald density limit and benefit from high-density operation thanks to the positive density dependence in the empirical energy confinement time scaling, $\tau_\mathrm{E} \propto n^{0.6}$ [6]. The fusion triple product, $n \cdot T \cdot \tau_\mathrm{E}$, thus has a more than linear dependence on density. Although first-principle plasma theory still cannot quantitatively explain these empirically found energy confinement times, it is well known that neoclassical transport, induced by the binary Coulomb collisions between the plasma particles, can cripple the confinement at high temperatures due to trapping particles in the helical ripple of a stellarator magnetic field. In the relevant $1/\nu$ -collisionality regime, the electron transport scales as $\varepsilon_\mathrm{eff}^{3/2} T_\mathrm{e}^{7/2}/(n_\mathrm{e} B_0^2 R_0^2)$ with the central magnetic field B_0 and the major radius R_0 of the fusion device [7]. Stellarator optimization addresses this issue by minimizing the effective helical ripple, ε_eff, which describes the influence of the 3D magnetic field geometry on the transport [8, 9]. The strong temperature scaling nevertheless necessitates low-temperature, high-density operation, which also has the advantage of reducing the slowing-down time of fusion-produced alpha particles, thereby minimizing possible losses and reducing the drive for energetic-particle instabilities [10].

Demonstrating stable high-density operation at fusion relevant plasma parameters for 30 minutes is one of the fundamental goals of the superconducting stellarator Wendelstein 7-X (W7-X) with a major radius of $R_0 = 5.5\,\mathrm{m}$ and a plasma volume of about $30\,\mathrm{m}^3$ [11, 12]. In contrast to tokamaks, plasma confinement of stellarators is intrinsically steady state, since the high-precision confining magnetic field is generated by external coils [13]. The magnetic field structure of W7-X is based on an optimized design aiming at overcoming the drawbacks of earlier stellarators [14]. The minimization of internal plasma currents already has been demonstrated at low density values of about $2 \cdot 10^{19}\,\mathrm{m}^{-3}$ [15]. This Letter addresses the first operation at high densities $> 10^{20}\,\mathrm{m}^{-3}$ in the $1/\nu$ -collisionality regime for which W7-X was optimized, which in conjunction with a steady-state heating scenario is the pre-requisite for achieving the envisaged 30-minutes discharges [16].

For plasma generation and heating in W7-X, a steady-state-capable electron-cyclotron-resonance heating (ECRH) system at 140 GHz was developed [17]. ECRH is the only method which allows highly localized power deposition without issues of plasma coupling and wave propagation, at least below the relevant cut-off densities. Moreover, the direct heating of the plasma elec-

* Torsten.Stange@ipp.mpg.de
† see [5] with full author list

trons mimics the conditions in a burning plasma, where the energetic alpha particles primarily transfer their energy to the electrons. In this Letter we also demonstrate that temperature equilibration between electrons and ions has been achieved in W7-X applying only ECRH in plasmas of sufficiently high density – similar to that of burning fusion plasmas. To propagate inside the plasma, the frequency of the electromagnetic waves must be above the plasma frequency. For the magnetic field of W7-X ($B_0 = 2.5\,\mathrm{T}$) and the plasma densities envisaged, this means that the design of the ECRH system had to be based on 2nd harmonic heating at $f = 140\,\mathrm{GHz}$ [17]. Because the incident microwave beams with a diameter of about 10 cm are fully absorbed at the resonance layer, X-mode polarization (X2-heating) is applied for plasma break-down and plasma heating below the X2 cut-off density ($< 1.2 \cdot 10^{20}\,\mathrm{m}^{-3}$). Approaching this cut-off, the polarization is changed to O-mode, which allows densities up to $\sim 1.8 \cdot 10^{20}\,\mathrm{m}^{-3}$ to be attained. Since an O-mode polarized microwave beam is not fully absorbed during a single passage through the plasma, an elaborate multi-pass absorption scheme for all ten microwave beams was developed and tested, demonstrating for the first time pure O2-heating beyond the X2 cut-off, giving access to the envisaged high density, $T_\mathrm{e} = T_\mathrm{i}$ regime of W7-X.

II. DESIGN OF THE HEATING SCENARIO

The design analysis needed to be conducted for only five of the ten ECRH-beamlines because of their symmetric arrangement with respect to the magnetic field of W7-X [17]. The design calculations were made with the ray-tracing code TRAVIS which includes the 3D-geometry of the magnetic field structure and allows to analyse the refraction of the beam as well as the radial distribution of the power deposition within the plasma [18]. The target plasma parameters chosen for the design analysis base on the first O2-heating tests during the first operational campaign with densities up to $n_\mathrm{e} = 0.4 \cdot 10^{20}\,\mathrm{m}^{-3}$ [19, 20]. In case of on-axis heating, the electron temperature profile is peaked with $T_\mathrm{e} = 3\,\mathrm{keV}$ in the plasma center and the density profile is expected to be flat with $n_\mathrm{e} = 1.2 \cdot 10^{20}\,\mathrm{m}^{-3}$, not considering possible effects of plasma fuelling with frozen hydrogen pellets [21]. Fig. 1a shows the absorption of the five individual O2-polarized beams (called Alpha, Bravo, Charly, Delta, Echo) as a function of the toroidal incidence angle, ϕ_0, between the beams and the normal of the magnetic axis. A maximum of about 80 % is predicted around $|\phi_0| = 17°$ which ideally should be achieved also for all subsequent beam passes through the plasma axis.

However, the steering capabilities of the ECRH-launchers and the plasma facing wall limit the possibility to use the optimal incidence angle. In W7-X the plasma facing wall opposite to the ECRH-launchers consists of graphite tiles with a size of typically $10\,\mathrm{cm} \times 10\,\mathrm{cm}$ which are mounted on an actively cooled CuCrZ-structure. A number of measures had to be implemented to make a multi-beam path layout steady-state capable. Firstly, the non-absorbed (shine-through) power after the first path has to centrally hit the tile to maximize the redirected power into the second path. Secondly, for graphite tiles the shine-through power after the first path is too high. With a microwave-absorption coefficient of $3 - 5\,\%$ [22] the tile would heat up to above 1000° in steady-state operation. Therefore, a molybdenum alloy (TZM) coated with tungsten is used as material, providing a very low absorption (0.3 %) and a good heat conductivity.

For two beamlines (Delta, Bravo) the shape of its particular reflector tile following the contour of the plasma-facing wall already directs the second path through the plasma axis and ends on a broad curved stainless steel panel located between the two ECRH launchers of the particular W7-X module. The large polished surface guarantees the reflection of the residual shine-through power into a third beam path for all five beams, even though beam refraction changes during plasma operation. The other three beams (Alpha, Charly, Echo) need special tiles for their first reflection on the inner side of the plasma facing wall. Providing the tiles with holographic grids on their reflecting surfaces, differing angles of incidence and reflection can be realized, directing also these beams through the magnetic axis again. This technique was first used at the tokamak ASDEX Upgrade to realize a two beam path O2-heating scenario. In contrast to the results reported here, they needed neutral beam injection in addition to the O2 ECRH to sustain the plasma at the desired densities [23].

The finally achieved angles ϕ_0 of the first paths are indicated in Fig. 1a by vertical lines. Especially the limiting steering capabilities are very restrictive for the Alpha beam as only an absorption of $< 50\,\%$ can be expected after the first pass at $B_0 = 2.5\,\mathrm{T}$. An additional way to optimise the absorption of ECRH power is to operate at higher magnetic field.

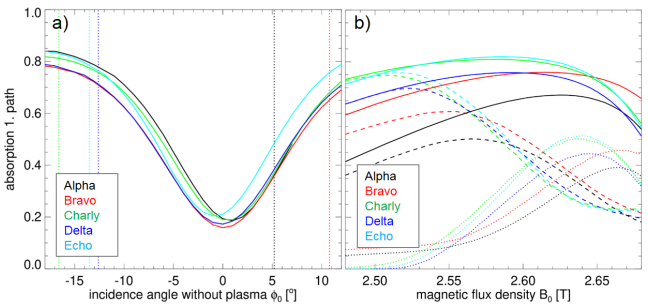

Figure 1. a) O2-absorption of the five individual beamlines versus the incidence angle ϕ_0 on the magnetic axis with $B_0 = 2.5\,\mathrm{T}$ in the bean shaped plane. The dashed vertical lines indicate the chosen incidence angles being a compromise between mirror steering and first wall geometry. b) O2-absorption of the 1st path versus the central magnetic field B_0. Dashed lines indicate the absorption by passing particles and dotted lines by trapped particles.

Due to the increase of the magnetic field B towards the inboard side of a toroidal confinement device and the relativistic effect ($\gamma = 1/\sqrt{1 - v^2/c^2}$) in the cyclotron resonance condition, $2\pi f - k_{||} v_{||} - n \cdot e \cdot B/m_e \gamma = 0$ [24], the energy of resonant electrons, E_{res}, is also increasing towards the inboard side involving cyclotron interaction of the Maxwellian tail of the electron distribution function. In case of a perpendicular wave vector to the magnetic field lines ($k_{||} = 0$) the resonance condition can be simplified to $E_{\mathrm{res}} = (n \cdot eB/2\pi m_e f - 1) m_e c^2$. However, the closer E_{res} is to the bulk electron temperature T_{e}, the higher the local absorption of the wave (necessary condition $E_{\mathrm{res}}/T_{\mathrm{e}} < 9$ [25]). In case of incomplete single-pass absorption and a peaked temperature profile, an increase of B_0 allows to maximize E_{res} by shifting the the end of the resonant path length to the plasma center and thus to higher T_{e}. Fig. 1b shows the absorption of the first beam path as a function of the central magnetic field. The optimum is reached at $B_0 = 2.6\,\mathrm{T}$, whereas the absorption is shifted towards the less well confined trapped particles. This will only have a small effect on the confinement, as the electron-electron energy relaxation time is $\tau_E^{\mathrm{ee}} \approx 1\,\mathrm{ms} \ll \tau_{\mathrm{E}}$ for an electron with 9 times higher energy compared to the bulk temperature.

To specify the overall absorption after three beam paths, the mode purity after redirecting the beams into the second and third path has to be taken into account. The holographic tiles in its present configuration preserve the polarization of the incoming wave. For this reason, the orientation of the tiles leads to a reflected wave which also has X-mode parts. However, after reflection at the cutoff-layer inside the plasma the X-mode part is again reflected at the high field side wall with about 50 % of the power turned back into O-mode, which can be considered as indirect absorption. For this reason, an overall absorption of about 93 % is expected, even though the overall direct O-mode absorption is only 88 %. As consequence, all W7-X diagnostics and other in-vessel plugins must be able to withstand a stray radiation level which corresponds to approximately 10 % of the total heating power. Assuming 10 MW as the reference power, all in-vessel components were designed to withstand a stationary stray-radiation level of $50\,\mathrm{kW/m^2}$ [17]. If this level of non-absorbed power turned out to be too high, a further upgrade could be polarization correcting holographic tiles to reduce the not absorbed power to about 2 % of the input beam power.

III. EXPERIMENTAL RESULTS

Fig. 2 shows a plasma achieving an extended phase of more than five energy confinement times above the X2-cutoff density only sustained by O2-heating and only limited by the capability of the pellet injector which was required to reach such high plasma densities. The main ingredients of this plasma were a carefully designed and tailored heating scenario, sufficiently high ECRH power, a higher magnetic field to maximize O2-absorption and pellet injection to reach high enough central plasma densities.

Plasma formation and the initial density rise were facilitated by helium, as increasing the density with helium turned out to be more reliable in W7-X divertor plasmas. The reasons are still not clear, however, for the presented ECRH scenario it is not relevant whether helium or hydrogen or a mixture of both are used. Plasma breakdown required X-polarization, in particular for the higher magnetic field, because the cold resonance was located off-axis at $r_{\mathrm{eff}}/a \approx 0.25$. After plasma formation, a rather quick transition to O-mode polarization was required because of the limited cooling capacity of the divertor, limiting the injected energy $\int Pdt$ to less than 80 MJ. At an average power of 5 MW this corresponds to a maximum plasma duration of 16 s. At $t = 0.2\,\mathrm{s}$ the density feedback system and six gyrotrons in O-mode polarization were activated. Even though the single path O2-absorption is only 20 %, the generated X-

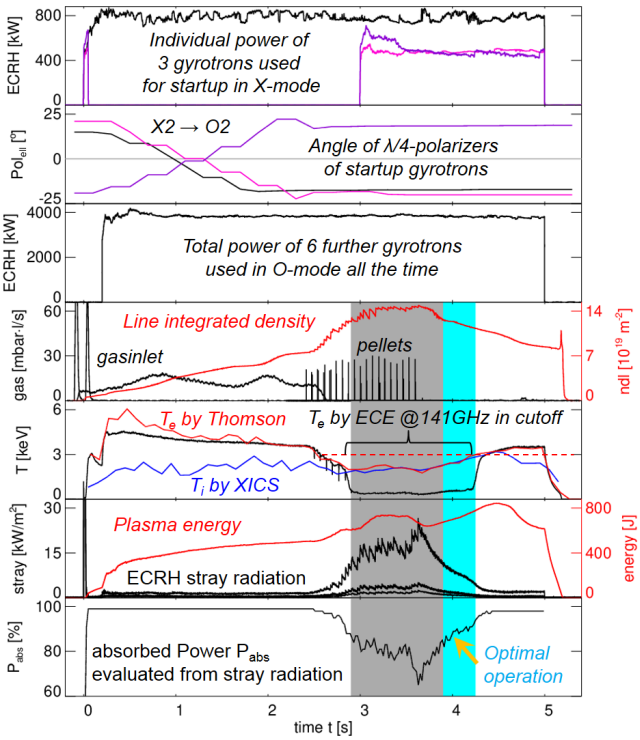

Figure 2. O2-heating scenario conducted at $B_0 = 2.62\,\mathrm{T}$. The both top traces indicate the total power and the polarization state of the 3 startup gyrotrons followed by the total power of the additional 6 gyrotrons operated exclusively in O-mode. The fourth timetrace shows the fuelling by gas puffing and pellets as well as the resultant line integrated density. The achieved electron and the ion temperatures in the fifth timetrace is overlaid with the ECE radiation temperature at 141 GHz indicating the X2-cutoff between $t = 2.9 - 4.3\,\mathrm{s}$. The two bottom time traces show the plasma energy, the ECRH stray radiation in module 2, 3 and 4 as well as the evaluated overall absorption.

mode part after the first and second reflection is fully absorbed. Even if the holographic tiles would perfectly convert the reflected power to O-mode (as planned for a later upgrade of the tiles), after the second beam path the stainless steel panel would reflect enough shine-through power in X-mode polarization to increase T_e, so that O2-absorption dominates for $t > 0.25\,s$. The main reason is the strong temperature dependence of the O2-mode absorption, which scales like $n_e(1 - n_e/n_{O\text{-cutoff}})^{3/2}T_e^2$ (in comparison to n_eT_e for an X2-polarized beam). Moreover, each ECRH beam is focused about 1.6 m behind its particular front steering mirror. As a result, the O-mode polarized shine-through power after the third path can be observed as footprint on the graphite tiles during this transient phase (shown in Fig. 3). Three absolutely calibrated stray radiation probes are utilized for the evaluation of the absorbed power in the vicinity of the ECRH launchers (see [26]). During the first 2 s of the density ramp-up phase the resulting overall absorption of the six gyrotrons, launching the microwaves in O-mode in a plasma below the X2-cutoff and considering the first four beam paths, is up to 99 %.

The initial density feedback was adjusted to a moderate increase of $3 \cdot 10^{19}\,m^{-3}s^{-1}$. During this period, there was enough time to turn the X-mode gyrotrons off, change the polarizers to O-mode, and turn them on again (at $t = 3\,s$). One gyrotron was kept operating during the polarization change to identify possible issues with arcing on the grooved polarizer mirrors. Once all polarizers were in O-mode, hydrogen pellet injection was applied to push the density above the X2-cutoff. The resulting density increase was accompanied by a drop of the central electron temperature to $T_e < 3\,keV$ (measured by the Thomson scattering diagnostic). The evolution of the radiation temperature T_{rad} of the second harmonic X-mode polarized electron cyclotron emission (ECE) near the gyrotron frequency clearly indicates the X2-cutoff in the plasma centre. As shown in Fig. 2 by the ECE channel at 141 GHz, at $t \approx 2.9\,s$ the T_{rad} drops to values close to zero when the cutoff is reached. At the same time the stray radiation level starts to increase (as indicated by the three stray radiation probes), caused by a combination of electron temperature decrease and the loss of the absorption of the X-mode contributions, originating from the microwave beam reflections of the multi-pass absorption scheme.

Even though the overall ECRH power was eventually increased to 5.6 MW (at $t = 3\,s$) by again turning on the two start-up gyrotrons, the electron temperature could not be increased to electron temperatures above 3 keV. As indicated by the grey shaded areas in Fig. 2 the maximum central density of $n_e = 1.3 \cdot 10^{20}\,m^{-3}$ (see Fig. 4) could be sustained for just about one second. Once the hydrogen pellets were spent and the density started to drop, the electron temperature increased again. Remaining in cut-off, the overall absorption increases from 70 % to 90 % as a result of the central T_e increasing to 3 keV (blue shaded area in Fig. 2). This value agrees very well with the predicted overall heating efficiency of at least 88 %. Although the goal is an absorption above 90 %, in the case shown here the absolute stray-radiation level always remained below the critical design value for W7-X in-vessel components of $50\,kW/m^2$.

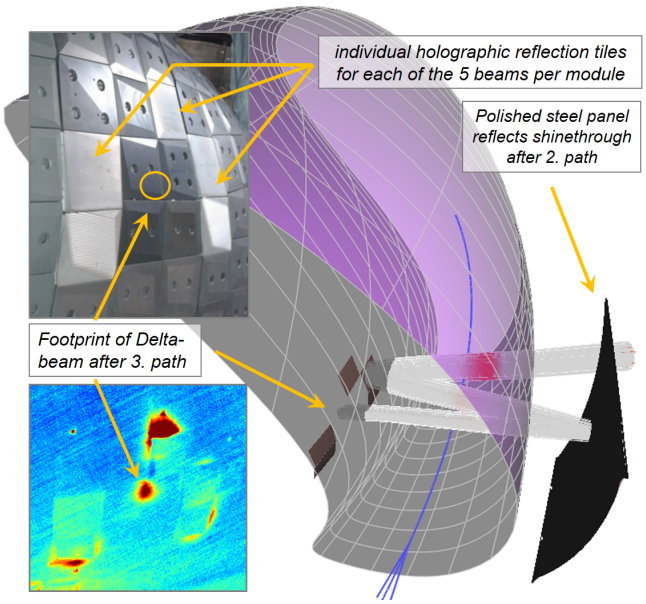

Figure 3. On the right side: 3D-visualization of the calculated triple pass of the Delta beam through the plasma in module 1. The plasma is visualized by its last closed fluxsurface (LCFS). On the left side: Infrared measurement at the end of an O2-heated discharge. In this example, the beam refraction was not accurately corrected because of an unexpected high density. For this reason, some graphite tiles around the reflector tiles heat up during the discharge. Furthermore, the relatively high shinethrough power of 2 %. of the Delta-beam even after the third path produces a clear infra-red footprint.

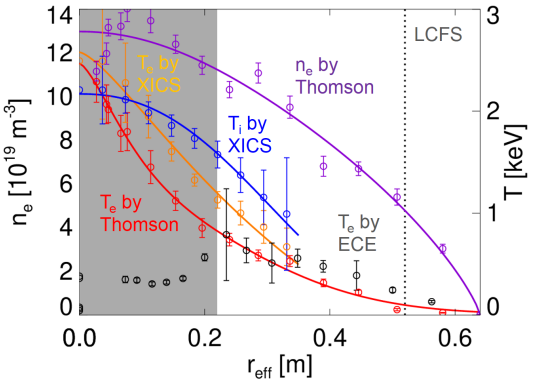

Figure 4. Radial profiles of electron density n_e, electron temperature T_e and ion temperature T_i measured during the period $t = 3.17 - 3.47\,s$ by Thomson Scattering, XICS (X-ray Imaging Crystal Spectrometer) and Electron Cyclotron Emission (ECE). The gray shaded area indicates the cutoff-region which is not accessible for an X2-polarized ECRH-beam.

A remarkable result of this O2-heating experiment is the full coupling of the electrons to the ions for electron densities $n_e > 10^{20}\,m^{-3}$ as indicated by the synchronous increase of the central T_e and T_i measured by two independent diagnostics in the time window of $t = 3.6 - 4.4\,s$. Moreover, peaked density profiles could be achieved by pellet fueling as shown in Fig. 4 for the density flattop phase.

IV. SUMMARY AND CONCLUSIONS

For the first time a high temperature plasma above the X2 density cutoff was sustained purely by O2-ECRH. Only by carefully designing the heating scenario and tailoring the plasma parameters, this demonstration could be achieved. This type of heating scenario is crucial for giving access to the $1/\nu$ collisionality regime for which W7-X was optimized. The high plasma densities, associated with this regime, lead to an equilibration of ion and electron temperatures, as already demonstrated by the example shown here. This means that ECRH alone, directly only heating the electrons, is sufficient to reach fusion relevant plasma parameters.

The underlying heating scenario utilized a multi-pass absorption scheme, based on three pre-defined beam paths. Compared to a simpler double beam path scenario, the main advantage is the low stray radiation level even in transient phases with low single path O2-absorption. The calculated beam propagation as well as the stray radiation levels are in good agreement with the experiment.

Increasing the ECRH power in the future will certainly help to access and reliably sustain the O2-heating above the X2-cutoff. Extending this phase will also depend on the availability of a new hydrogen pellet injector, capable of delivering more pellets over a longer period of time. The overall beam absorption can be improved by further optimizing the holographic reflector tiles, also correcting the polarization of the reflected beams. In addition, realizing a fourth beam path, by replacing the affected carbon tiles by tungsten covered TZM tiles, would lead to improving the heating efficiency even further.

ACKNOWLEDGMENTS

This work has been carried out within the framework of the EUROfusion Consortium and has received funding from the Euratom research and training programme 2014 - 2018 under grant agreement No 633053. The views and opinions expressed herein do not necessarily reflect those of the European Commission.

[1] M. Greenwald, Plasma Phys. Control. Fusion **44**, R27 (2002).
[2] M. Keilhacker et al., Nucl. Fusion **39**, 209 (1999).
[3] L. D. Horton et al., Nucl. Fusion **39**, 993 (1999).
[4] J. D. Strachan et al., Phys. Rev. Lett. **72**, 3526 (1994).
[5] S. Ishida et al., Nucl. Fusion **39**, 1211 (1999).
[6] H. Yamada et al., Nucl. Fusion **45**, 1684 (2005).
[7] C. D. Beidler et al., Nucl. Fusion **51**, 076001 (2011).
[8] W. Dommaschk et al., Nucl. Fusion **24**, 794 (1984).
[9] C. D. Beidler et al., Plasma Phys. Control. Fusion **36**, 317 (1994).
[10] P. Helander et al., Plasma Phys. Control. Fusion **54**, 124009 (2012).
[11] C. Beidler et al., Fusion Technol. **17:1**, 148 (1990).
[12] V. Erckmann et al., in *17th IEEE/NPSS Symposium Fusion Engineering (Cat. No.97CH36131)* (San Diego, USA, 1997).
[13] T. Sunn Pedersen et al., Nat. Commun. **7** (2016).
[14] G. Grieger et al., Phys. Fluids B **4**, 2081 (1992).
[15] A. Dinklage et al., Nature Physics **14**, 855 (2018).
[16] T. Sunn Pedersen et al., Physics of Plasmas **24**, 055503 (2017).
[17] V. Erckmann et al., Fusion Sci. Technol. **52**, 291 (2007).
[18] N.B. Marushchenko et al., Comput. Phys. Commun. **185**, 165 (2014).
[19] R.C. Wolf et al., Nucl. Fusion **57**, 102020 (2017).
[20] T. Stange et al., EPJ Web Conf. **157**, 02008 (2017).
[21] J. Baldzuhn et al, Fusion Sci. Technol. **46**, 348 (2004).
[22] W. Kasparek. et al., International Journal of Infrared and Millimeter Waves **22**, 1695 (2001).
[23] H. Hoehnle et al., Nucl. Fusion **51**, 083013 (2011).
[24] V. Erckmann et al., Plasma Phys. Control. Fusion **36**, 1869 (1994).
[25] A. G. Shalashov et al., Plasma Physics Reports **32**, 480 (2006).
[26] D. Moseev et al., Nucl. Fusion **57**, 036013 (2017).